

Received Date : 05-Aug-2016

Revised Date : 19-Oct-2016

Accepted Date : 23-Nov-2016

Article type : Research Article

Reactivity of 9-aminoacridine drug quinacrine with glutathione limits its anti-prion activity

Short running title: “**Glutathione reduces quinacrine effects on prions**”

Martin Šafařík,^{a,#} Tibor Moško,^{b,#} Zbigniew Zawada,^a Eva Šafaříková,^b Martin Dračínský,^a Karel Holada,^b Jaroslav Šebestík^{a,*}

^a*Institute of Organic Chemistry and Biochemistry, Academy of Sciences of the Czech Republic, v.v.i., Flemingovo nám. 2, 166 10 Prague 6, Czech Republic;*

^b*Institute of Immunology and Microbiology, First Faculty of Medicine, Charles University in Prague, Studničkova 7, 128 00 Prague 2, Czech Republic*

Corresponding Author

*E-mail: jsebestik@seznam.cz. Phone: (+420)220-183-445. Fax: (+420)224-310-090.

This article has been accepted for publication and undergone full peer review but has not been through the copyediting, typesetting, pagination and proofreading process, which may lead to differences between this version and the Version of Record. Please cite this article as doi: 10.1111/cbdd.12918

This article is protected by copyright. All rights reserved.

Author Contributions

[#]M.Š. and T.M. contributed equally. Z.Z. provided reference sample of GlutQui and data for previous way of preparation. E.Š. provided recombinant prion protein for fluorescence assays. M.D. measured NMR spectra. K.H. and J.Š. designed the experiments and wrote the manuscript.

KEYWORDS: quinacrine, failure in clinical trials, nucleophilic displacement, prion-protein binding, anti-prion activity

ABSTRACT: Quinacrine – the drug based on 9-aminoacridine – failed in clinical trials for prion diseases, whereas it was active in *in-vitro* studies. We hypothesize that aromatic nucleophilic substitution at C9 could be contributing factor responsible for this failure because of the transfer of acridine moiety from quinacrine to abundant glutathione. Here, we described the semi-large-scale synthesis of the acridinylated glutathione and the consequences of its formation on biological and biophysical activities. The acridinylated glutathione is one order of magnitude weaker prion protein binder than the parent quinacrine. Moreover, according to $\log D_{pH\ 7.4}$ the glutathione conjugate is two orders of magnitude more hydrophilic than quinacrine. Its higher hydrophilicity and higher dsDNA binding potency will significantly decrease its bioavailability in membrane-like environment. The glutathione deactivates quinacrine not only directly but also decreases its bioavailability. Furthermore, the conjugate can spontaneously decompose to practically insoluble acridone, which is precipitated out from the living systems.

1. Introduction

9-Aminoacridines are important compounds used for the treatment of cancer, viruses and neurodegenerative diseases (1-3). Quinacrine (**1**) is perhaps one of the most important drugs from the family of 9-aminoacridines. It is used for the treatment of various diseases such as *rheumatoid arthritis*, *lupus erythematosus*, chloroquine-resistant malaria, tapeworm infections (*Taenia saginata*), Chagas disease, and epilepsy (refractory *petit mal*) (4-8). In *in-vitro* experiments quinacrine diminished the propagation of prions in cell culture, suggesting that the drug can be used for treatment of patients with Creutzfeldt-Jakob disease or the new variant of this disease (5). Bis-acridinylated compounds were tested not only for their anti-prion activity (9) but also for their anti-Alzheimer's activity (10). Although quinacrine demonstrated excellent *in-vitro* results (5), it failed in clinical trials (11,12) and did not prolong survival in a murine model of Creutzfeldt-Jakob disease (13) or in naturally scrapie infected sheep (14). Firstly, the failure of quinacrine *in-vivo* was explained by selection of quinacrine resistant prions during the treatment (15). In game model, the application of quinacrine even seemed to accelerate conformational change and spreading of chronic wasting disease prions (16). Secondly, the failure was correlated with clearance of quinacrine from the brain (17). Despite quinacrine reached a brain in concentration corresponding to 10-fold of EC_{50} of *in-vitro* test (18), quinacrine was rapidly cleared by P-glycoprotein efflux transporter (17). MDR^{0/0} mice, deficient in P-glycoprotein multi-drug resistance (MDR) transporter, can accumulate up to 100 μ M of quinacrine in the brain. Such a high concentration of quinacrine leads to only temporal decrease of abnormal prion protein (PrP^{Sc}) in brains of infected mice and gradually increases after several days despite the presence of the drug (15). Thirdly, the lack of quinacrine efficiency *in-vivo* may have pharmacodynamic origin as quinacrine is capable to limit formation of new molecules of PrP^{Sc}, but does not affect already existing PrP^{Sc} (19).

As we have previously shown, quinacrine reacts with thiol-containing peptides including glutathione (GSH) with which it forms *S*-acridinylated product – GlutQui (20) (Figure 1). We hypothesize that this could be another factor responsible for quinacrine failure in clinical trials. The failure can be then explained by different levels of GSH in neuronal cell cultures (5) and in prion infected brains with increased amount of astrocytes (21). Especially, astrocytes not only contain higher levels of GSH than neurons, but also release significant amounts of GSH into the extracellular space (22). A better understanding of the quinacrine anti-prion limits can facilitate drug design of *in-vivo* active compounds based on acridine structure.

In order to corroborate our hypothesis, we studied the influence of acridine moiety transfer on various biological and biophysical parameters. The prion protein binding affinity, distribution between aqueous and organic phase, dsDNA binding activity and *in-vitro* anti-prion activity were evaluated.

2. Methods and Materials

2.1. General Procedures

All reagents were analytical grade and were purchased from Sigma-Aldrich, Czech Republic, unless stated otherwise. During the syntheses, the molecular weights of the peptide conjugates were determined using ESI-MS (Bruker Daltonics Reflex IV and Waters Q-Tof micro instruments). Agilent 1200 instrument (Santa Clara, CA, USA) with a quaternary pump, thermostat, diode array detector and a reversed-phase C₁₈ column (PoroShell 120 SB-C₁₈ 2.7 μm, 3x50 mm, Agilent Technologies, Santa Clara, CA, USA) were used for HPLC using acetonitrile (ACN) gradient from 1-1-13-19-57-100% within 0-1-2-8-13-15 min. The column was

Accepted Article

thermostated to 40 °C. Unless stated otherwise, water for HPLC was modified with 0.1% trifluoroacetic acid (TFA). UV-Vis spectra were acquired using a Varian Carry 5000 instrument (Palo Alto, CA, USA) with a quartz cell (1 cm). NMR spectra of dimethylsulfoxide-*d*₆ (DMSO-*d*₆) solutions were recorded with a Bruker Avance III spectrometer equipped with a 5-mm diameter cryoprobe operating at 600.1 MHz for ¹H and 150.9 MHz for ¹³C. The signals were referenced to residual solvent signals (δ = 2.50 and 37.9 ppm in ¹H and ¹³C, respectively). Resonance assignment of all signals was obtained by a combination of 1D and 2D (H,H-COSY, H,C-HSQC, H,C-HMBC) experiments.

2.2. Syntheses of *S*-(6-Chloro-2-methoxyacridin-9-yl)glutathione acetate (**3a**) and

S-(6-Chloro-2-methoxyacridin-9-yl)glutathione hydrochloride (**3b**)

The compounds were prepared similarly to procedure published previously, but the purification steps were significantly improved (20). GSH (1 g, 3.25 mmol) and quinacrine dihydrochloride (1.54 g, 3.25 mmol) were dissolved in 45 mL of water. The pH was adjusted by 1M NaOH to 7.5. The solution was stirred and heated at 37 °C for 6 h. The conversion was approximately 80%; however, the prolonged reaction time did not provide significant improvement of conversion. Small sample (150 mg) of the reaction mixture was purified by RP-HPLC using gradient from 5%-100% ACN within 40 min. The TFA salt was converted to acetate by repeated dissolution in 5% acetic acid (AcOH) and freeze drying. The yield was 30 mg (1%) of **3a**. According to mixed inject method, the product was identical with the previously published one. HPLC RT 7.8 min. ESI HRMS (m/z): for [M+H]⁺ C₂₄H₂₆O₇N₄ClS calcd. 549.12052; found 549.12058 (0.10695 ppm). ESI HRMS neg. (m/z): for [M-H]⁺ C₂₄H₂₄O₇N₄ClS calcd. 547.10597; found 547.10486 (-2.03310 ppm). ¹H-NMR is almost identical to that of **3b** reported

below with one extra signal at 1.91 ppm belonging to acetate. One half of the crude reaction mixture was loaded on weak anion exchanger (Zerolit G, SRA97, 100 mL) in hydroxide cycle. The unreacted quinacrine was removed by washing with water (ca 300 mL) till the eluent is colorless. Most of the quinacrine was eluted with water; however, a small amount of quinacrine remained bound to the ionex even after 2 days elution as checked in another experiment. Then free unreacted GSH was recovered by fractional elution with 5% acetic acid (ca 400 mL). According to analytical HPLC, it was contaminated with desired product **3a**. When the free GSH was removed, the product **3b** was eluted with 0.5M HCl (ca 150 mL). After evaporation and drying in vacuum at 40 °C over night, it provides orange solid **3b** with yield 300 mg (14%) of HPLC pure compound. According to mixed inject method, the product was identical with previously published one. HPLC RT 7.8 min. For $C_{24}H_{25}N_4O_7S_4Cl$ (548.11) found ESI-MS, m/z: 549.1 (M+H)⁺. The Zerolite G was regenerated with 1M HCl and 1M NaOH and second half of the reaction mixture was purified. Yield 205 mg (9%). The total preparative yield of **3b** was 23%. For [H- γ -Glu-Cys(Qui)-Gly-OH]₄ · 9 HCl · 9 H₂O (C₉₆H₁₂₇N₁₆O₃₇S₄Cl₁₃) calc. 42.92% C, 4.77% H, 8.34% N, 4.77% S, 17.16% Cl; found: 43.17% C, 4.42% H, 8.04% N, 4.80% S, 17.49% Cl. ESI HRMS neg. (m/z): for [M-H]⁺ C₂₄H₂₄O₇N₄ClS calcd. 547.10597; found 547.10486 (-2.03310 ppm). ¹³C NMR: 171.1 (Glu- δ), 171.0 (Gly-C'), 171.0 (Glu-C'), 170.0 (Cys-C'), 158.2 (C2), 146.3 (C4b), 146.1 (C4a), 139.5 (C9), 134.1 (C6), 131.9 (C4), 130.0 (C8b), 18.7 (C8), 128.2 (C5), 128.0 (C7), 127.3 (C8a), 126.3 (C3), 102.4 (C1), 55.9 (OCH₃), 53.2 (Cys- α), 51.8 (Glu- α), 40.8 (Gly- α), 38.8 (Cys- β), 30.8 (Glu- γ), 26.0 (Glu- β). ¹H NMR: 8.67 (d, 1H, $J_{8,7} = 9.3$, H-8), 8.41 (d, 1H, $J_{NH,\alpha} = 8.3$, Cys-NH), 8.37 (t, 1H, $J_{NH,\alpha} = 5.9$, Gly-NH), 8.23 (bs, 3H, NH₃⁺), 8.23 (d, 1H, $J_{5,7} = 2.2$, H-5), 8.12 (d, 1H, $J_{4,3} = 9.4$, H-4), 7.90 (d, 1H, $J_{1,3} = 2.8$, H-1), 7.69 (dd, 1H, $J_{7,8} = 9.3$, $J_{7,5} = 2.2$, H-7), 7.61 (dd, 1H, $J_{3,4} = 9.4$, $J_{3,1} = 2.8$, H-3), 4.41 (ddd,

1H, $J_{\alpha,\text{NH}} = 8.3$, $J_{\alpha,\beta} = 9.4$ and 4.6, Cys- α), 4.02 (s, 3H, OCH₃), 3.90 (m, 1H, Glu- α), 3.59 (d, 2H, $J_{\alpha,\text{NH}} = 5.9$, Gly- α), 3.34 (dd, 1H, $J_{\text{gem}} = 13.4$, $J_{\beta,\alpha} = 4.8$, Cys- β), 3.19 (dd, 1H, $J_{\text{gem}} = 13.4$, $J_{\beta,\alpha} = 9.4$, Cys- β), 2.18–2.25 (m, 2H, Glu- γ), 1.91–2.00 (m, 2H, Glu- β). ¹H-NMR and ¹³C-NMR agreed with previously published one (20). For copies of spectra see Supplementary Information (Figures S3 and S4 for NMR, and Figures S6 and S7 for HRMS spectra). We have observed concentration dependent decomposition of **3b** in DMSO-*d*₆ with traces of water.

2.3. Reactivity of 9-aminoacridines with GSH

9-Aminoacridine (230 mg, 1 mmol) or tacrine (234 mg, 1 mmol) and GSH (307 mg, 1 mmol) were stirred in phosphate buffer (50 mM, pH 7.5, 100 mL) at 37 °C under Ar for 24 h. The progress of reaction was monitored by analytical HPLC in gradient from 5%-100% ACN within 20 min. Neither 9-aminoacridine nor tacrine were consumed by chemical reaction.

2.4. Stability of GlutQui in buffer and DMSO

Corresponding amount of GlutQui (**3b**, 0.5-50 mg) was dissolved in 1 mL of medium (either phosphate buffer 0.1 M, pH 7.5 or neat DMSO) and maintained under Ar at 37 °C for 7-10 days. Concentrations of GlutQui and decomposition products were determined using HPLC in gradient 5-5-100% CH₃OH within 0-1-11 min with flow 1 ml/min, thermostated Poroshell 120 EC-C18 2.7 μm , 3.0x50 mm column at 40 °C. The decomposition products were also characterized by NMR spectroscopy. Compounds **2** and **4** were identified in the decomposition mixture in 1:1 ratio. GSH (**2**) ¹³C NMR: 171.4 (Glu- δ), 171.1 (Gly-C'), 170.9 (Glu-C'), 170.5 (Cys-C'), 51.9 (Cys- α), 51.8 (Glu- α), 41.0 (Gly- α), 39.9 (Cys- β), 30.9 (Glu- γ), 26.1 (Glu- β). ¹H NMR: 8.44 (m, 3H, NH₃⁺), 8.41 (d, 1H, $J_{\text{NH},\alpha} = 8.5$, Cys-NH), 8.37 (t, $J_{\text{NH},\alpha} = 5.9$, Gly-NH), 4.58 (ddd, 1H, $J_{\alpha,\text{NH}}$

= 8.5, $J_{\alpha,\beta}$ = 9.9 and 4.2, Cys- α), 3.91 (m, 1H, Glu- α), 3.75 d, 2H, $J_{\alpha,\text{NH}}$ = 5.9, Gly- α), 3.13 (dd, 1H, J_{gem} = 13.5, $J_{\beta,\alpha}$ = 4.2, Cys- β), 2.87 (dd, 1H, J_{gem} = 13.5, $J_{\beta,\alpha}$ = 9.9, Cys- β), 2.43 (m, 1H, Glu- γ), 2.33 (m, 1H, Glu- γ), 1.98–2.09 (m, 2H, Glu- β). 6-Chloro-2-methoxyacridin-9(10*H*)-one (**4**)
 ^{13}C NMR: 175.8 (C-8), 154.5 (C-2), 141.4 (C-4b), 137.8 (C-6), 135.9 (C-4a), 128.5 (C-8), 124.7 (C-3), 121.4 (C-8b), 121.3 (C-7), 119.6 (C-4), 118.4 (C-8a), 116.5 (C-5), 105.2 (C-1), 55.6 (OCH₃). ^1H NMR: 12.23 (s, 1H, H-10), 8.21 (d, 1H, $J_{8,7}$ = 8.7, H-8), 7.63 (d, 1H, $J_{5,7}$ = 2.0, H-5), 7.60 (d, 1H, $J_{1,3}$ = 3.0, H-1), 7.58 (d, 1H, $J_{4,3}$ = 8.9, H-4), 7.42 (dd, 1H, $J_{3,4}$ = 9.0, $J_{3,1}$ = 3.0, H-3), 7.22 (dd, 1H, $J_{7,8}$ = 8.7, $J_{7,5}$ = 2.0, H-7), 3.85 (s, 3H, OCH₃). Copies of NMR spectra after decomposition are depicted in Figure S5.

2.5. Solubility of 9-aminoacridines in water

To a sample of 9-aminoacridines (50 mg) was consecutively added 50 μL of solvent. The suspension was sonicated for 5 min and evaluated by naked-eye with magnifying glass for transparency. When undissolved particles remained, another portion of solvent was added. When the sample was solubilized in volume lower than 100 μL of solvent, it was evaporated to dryness and after the first 50 μL the process was repeated with 5 μL step. For sparingly soluble compounds, only 1 mg was used for the assay.

2.6. Acridine-prion binding assay

The recombinant full length mouse prion protein with *N*-terminal His tag (His-mPrP23-231) was prepared and purified as described previously (20,23). The assay based on quenching of prion-protein intrinsic fluorescence was adapted according to previous work (24). The intrinsic fluorescence of His-mPrP23-231 (6 μM) in phosphate buffer (10 mM, pH 8) was quenched by

increasing concentration of acridine compound using a Jasco FP-6600 spectrofluorimeter with excitation at 295 ± 3 nm (wavelength in which the filter effect caused by investigated acridines was negligible) and emission at 337 ± 2 nm at 18°C . The fluorescence data were acquired 5 min after the ligand addition in order to achieve ligand-protein equilibrium. Fluorescence of the same system without prion protein was subtracted from the corresponding experiment. Non-linear regression analysis was used for suppression of experimental errors using program xmgrace (<http://plasma-gate.weizmann.ac.il/Grace/>) and fitting with exponential function:

where F_{max} was the fluorescence intensity of the native His-mPrP23-231 in the absence of each compound, F_∞ was a theoretical value for complete saturation of all binding sites, and QC_{50} was the concentration of acridine species causing 50% quenching of prion-protein fluorescence. This function and equation 2 were used for generation of 1000 data points with inverse fractional saturation ($1/\Delta F$) as a dependent value and ligand concentration as an independent value.

The constructed data were fitted with the rectangular hyperbolic equation:

where K_D was dissociation constant.

2.7. Apparent distribution coefficients of acridines between *n*-octanol-buffer phase

The apparent distribution coefficients were obtained by shake-flask method (25,26). Briefly, aqueous phosphate buffer (10 mM, pH 7.4, 250 mL) and *n*-octanol (250 mL) were well shaken and let stand overnight at 6°C to separate as saturated phases. Prior to distribution experiment 5 mL of each of saturated phases were intensively mixed with 16 μmol acridine compound overnight at 6°C . The low temperature was used in order to prevent hydrolysis of acridines to

Accepted Article

corresponding acridones (20,27). The phases were separated by centrifugation and examined by UV-Vis spectroscopy at 18 °C. The absorbances at 400, 402, and 420 nm were used for calibration curves and quantification of acridines in the both saturated phases. The average of concentrations determined in each wavelength was used. When the absorbance was above 1, the aliquot of the phase was diluted and reexamined.

2.8. Acridine-dsDNA interaction assay by displacement of ethidium bromide

An ethidium-DNA complex was formed by mixing 1.27 μM solution of ethidium bromide and 0.696 μM (in base pairs) of calf thymus-DNA (CT-DNA). Measurements were carried out in 3 mL of phosphate buffer (50 mM, pH 7.4, 18 °C). Small volumes of a concentrated solution of inhibitor were then titrated while the fluorescence of the solution was monitored with excitation at 546 ± 3 nm and emission at 600 ± 2 nm. Fluorescences were read at least 3-times and average values were used. Fluorescence of the same system without ethidium was subtracted from the corresponding experiment. Nonlinear curve fitting was used to determine IC_{50} values by fitting the raw displacement data to a one-phase exponential decay curve using xmgrace software utilizing modified equation 1. QC_{50} value was substituted with IC_{50} – the concentration of inhibitor causing 50% displacement of ethidium bromide.

The conversion (28,29) of IC_{50} values to corresponding K_i (apparent inhibition constant) is based on Eqs. (4-6),

where [NA] is the concentration of “free” (unbound) nucleic acid, [Obs] is the concentration of the “free” observable species (ethidium), [NA–Obs] is the concentration of the NA–Obs complex, [I] is the concentration of “free” inhibitor, and [NA–I] is the concentration of inhibitor-bound nucleic acid. This calculation assumes that one equivalent of inhibitor displaces one

equivalent of ethidium and thus the term “apparent” affinity is used. According to the ethidium–CT-DNA association curve, the $K_D = 0.88 \mu\text{M}$ and the binding stoichiometry is 0.46 ethidium binding sites per base pair (n). Upon adding $0.696 \mu\text{M}$ of CT-DNA to $1.27 \mu\text{M}$ of ethidium, the concentration of ethidium–DNA [NA–Obs] = $0.18 \mu\text{M}$, free ethidium [Obs] = $1.09 \mu\text{M}$, and free DNA [NA] = $0.14 \mu\text{M}$ (in available binding sites). Upon titration of the inhibitor to its IC_{50} value, the concentration of the complex [NA–Obs] = $0.09 \mu\text{M}$, free ethidium [Obs] = $1.18 \mu\text{M}$, free DNA [NA] = $0.14 \mu\text{M}$ (in available binding sites), [NA–I] = $0.09 \mu\text{M}$, and the concentration of free inhibitor [I] = $\{(IC_{50} \text{ value}) - [\text{NA–I}]\}$. These values were used to solve Eq. (6).

2.9. Cell line and prion strain

As a model of prion infection, we used prion sensitive CAD5 cells (Cath.a-differentiated cell line) (30) provided by Charles Weissmann (Department of Infectology, Scripps Research Institute, FL, USA). CAD5 cells were chronically infected with Rocky Mountain Laboratory (RML) strain of mouse-adapted scrapie prions as described previously (31). Cells were maintained in Opti-MEM medium supplemented with 10% bovine growth serum and penicillin/streptomycin (Invitrogen).

2.10. Toxicity and cell culture manipulation

Stock solution of quinacrine (5 mM) was prepared in phosphate-buffer saline (PBS) pH 7.4 and GlutQui (**3b**) was dissolved in DMSO (85 mM solution). In the first round of experiments, the stock solution was used during the course of the experiment, in the second round of experiments, the solutions were prepared fresh each day to eliminate the effect of above mentioned decomposition of GlutQui. Prior to testing anti-prion activity, the toxicities of quinacrine and

Accepted Article

GlutQui towards CAD5 cells were evaluated and the concentrations which did not prevent the growth of the cells were determined. Based on the toxicity testing the concentrations 0.3 - 4 μM and 10 -200 μM were used for quinacrine and GlutQui, respectively. Chronically RML infected or non-infected CAD5 cells (70,000 cells) were seeded per tissue culture dish (10 cm in diameter) to ensure enough space for cells to growth for at least 7 days. Medium with quinacrine or GlutQui was exchanged every day for continuous treatment or the acridine was applied only once at first day for “one dose” treatment (acridine free medium was then changed every day). At 7th day, the cells were quantitatively harvested and counted. For toxicity measurement, the LC_{50} values were determined using equation analogous to Eq. (1). However, the number of cells equivalent to “ F_{∞} ” parameter was fixed to be zero. From every tissue culture dish, 110,000 cells were used for standard scrapie cell assay (SSCA) and the rests of cells were washed in PBS and pellets were stored at -80°C for western blot analysis.

2.11. Standard Scrapie Cell Assay

The samples were investigated by SSCA (32). All steps were carried out at room temperature unless stated otherwise. The ELISPOT plates (Multiscreen 96 well filter plates with high protein binding Immobilon-P membrane, 0.45 μm , Millipore) were activated with 60 μL of 70% ethanol per well. The ethanol was removed by vacuum. Wells were washed twice by 160 μL PBS and 50 μL of PBS was added to each well to prevent drying out. Cells were washed and diluted in PBS to 100,000 and 10,000 cells per ml and 100 μL aliquots plated to the wells of ELISPOT plate in eightplicates (10,000 or 1,000 cells per well). Cells were immobilized to the membrane by vacuum (Supelco) and drying the ELISPOT plates at 50 °C for 1 hour. Plates were stored at 4 °C for up to two weeks before further processing.

For proteinase K (PK) treatment, 60 μ L of PK (2 μ g/mL) were added to each well and incubated at 37 °C for 30 minutes. After 30 minutes, cells were washed with 160 μ L of PBS and the PK was inhibited by 2 mM phenylmethanesulfonyl fluoride (PMSF) in PBS for 10 minutes. Subsequently, cells were washed with 160 μ L of PBS and denatured by treatment with 150 μ L of 3 M guanidine thiocyanate in 10 mM tris(hydroxymethyl)aminomethane (TRIS)-HCl, pH 8 for 10 minutes. After denaturation, the cells were washed 4 times with 160 μ L of PBS and the membrane was blocked using Superblock solution (Pierce) for 1 hour. Blocking reagent was removed and primary antibody (60 μ L per well, 6D11 Covance) in TRIS buffered saline pH 7.4 with 0.05% Tween 20 (TBS-T) and 1% non-fat milk (Biorad) was added and incubated for 2 hours. Cells were washed 4 times with TBS-T and incubated with 60 μ L of secondary antibody (Alkaline phosphatase conjugated affinity purified F(ab')₂ fragment DAM IgG, Jackson) for 1 hour. The cells were washed 5 times with TBS-T and developed with AP Conjugate Substrate Kit (Bio-Rad). Spots on ELISPOT plates were quantified using the Nikon system equipped with analytical software (NIS-Elements, ver. 4.20). The SSCA data were fitted by equation analogous to Eq. (1). However, the number of spots equivalent to “ F_{∞} ” parameter was fixed to be zero.

2.12. Western blot

Cell pellets were lysed using protein lysis buffer (50 mM TRIS pH 7.4, 150 mM NaCl, 0.5% Triton X-100, and 0.5% Na deoxycholate) on ice for 30 minutes with occasional vortexing. Cell nuclei were not excluded from lysates and samples were treated with benzonase (Novagen). Protein concentrations were determined using bicinchoninic acid assay (Pierce) according to manufacturer's instructions. For samples not treated with PK, 30 μ g of total protein was loaded on gel per line. For samples treated with PK, 300 μ g of total proteins was incubated with 50

Accepted Article

$\mu\text{g/ml}$ of PK for 30 minutes at 37 °C. The PK treatment was stopped by adding PMSF to final concentration 2 mM for 10 minutes. Proteins were precipitated (salting-out in presence of 10% NaCl and 0.05% *N*-lauroyl sarcosine Na) on ice (33), washed 2 times in 25 mM TRIS-HCl pH 8.8 and dissolved in Laemmli sample buffer. Gel electrophoresis and blotting was performed as described previously (34). The membranes were developed after probing with a mix of mAbs AH6 (epitope PrP159–174, Roslin Institute, Midlothian, UK) and DC2 (epitope PrP39–46, provided by Vladka Curin-Serbec, Blood Transfusion Centre of Slovenia, Ljubljana).

3. Results

3.1. Semi-large-scale synthesis of quinacrine—GSH conjugate

In order to avoid expensive HPLC separation, ionex chromatography with Zerolit G weak anion exchanger was used for separation of reaction mixture after acridinylation of GSH (20). The unconsumed quinacrine (base) is almost not retained by the ionex. The removal of unreacted GSH from GlutQui was done by various strength of acid used for elution. AcOH was sufficient for elution of mixture of the GSH contaminated with small amount of its conjugate **3a**. Stronger acid (HCl) was used for final release of the conjugate **3b** from the resin in more than 95% purity. The new synthesis provides hundreds of milligrams of the peptide conjugate, which allows most of biological and physicochemical assays.

3.2. Resistance of primary 9-aminoacridines towards thiols

In contrast to quinacrine, both 9-aminoacridine and tacrine remained stable during incubation with GSH within 24 h at 37 °C under Ar.

3.3. Stability of GlutQui

In order to investigate biological properties of GlutQui (**3b**), it was important to know whether GlutQui is stable under physiological conditions, as well as, in stock solution. Within the 7 days, the concentration of GlutQui did not change more than 1% in buffer and more than 3% in DMSO, when the starting concentration was lower than 1 mg/mL. However, the situation became different when the initial concentration of GlutQui was increased. In DMSO, almost complete decomposition was achieved within few days with starting concentration higher than 15 mg/mL (Figure 2).

According to NMR study, the GlutQui (**3b**) decomposes to GSH (**2**) and corresponding acridone (**4**). Interestingly, measurement of NMR spectra of pure compounds requires the utilization of low sample concentration ca 1.5 mg/mL and employment of CryoProbe. Otherwise partial decomposition takes place (Figure S1 in Supplementary Information).

3.4. Prion-binding of the acridines

Binding of His-mPrP23-231 with various acridines was investigated by assay of Villa et al. (24). This assay revealed that quinacrine is more than 20-times stronger binder than the GlutQui (Figure 3 and Table 1). The conjugation with GSH led to 95% deactivation of quinacrine. Consequently, the GlutQui conjugate **3a** is more than 3-times weaker prion protein binder than unsubstituted 9-aminoacridine.

3.5. Bioavailability of the acridines

Two factors influencing bioavailability of 9-aminoacridines were evaluated i.e. DNA binding and distribution between *n*-octanol/buffer system. When GSH accepts acridine moiety from quinacrine, the DNA affinity increases ca 5-folds (Table 2). The GlutQui conjugate **3a** is ca 21-times tighter DNA binder than 9-aminoacridine.

Reaction of GSH with quinacrine increased water solubility (with exception of dihydrochloride salt **3b**); however, decreased membrane permeability (Table 3, Table 4). Quinacrine easily penetrates to organic phase, whereas GlutQui conjugate **3a** is mostly located in aqueous one, i.e. the GlutQui prefers to stay in aqueous phase two orders of magnitude more than the original drug.

3.6. Toxicity and anti-prion activity of the acridines

The assay in dividing prion permissive CAD5 cells was established. The toxic effects such as mainly observed inhibition of cell divisions and almost unseen detachment of dead cells in culture were noticeable at 0.3 μM concentration of quinacrine and 30 μM concentration of GlutQui (Figure 4). Calculated values of LC_{50} under the culture condition setup were 1.3 μM and ≥ 97 μM for quinacrine and GlutQui (**3b**), respectively.

The efficacy of prion clearance from the cells was investigated by standard scrapie cell assay (SSCA) (32) (Figure 5). The concentrations of quinacrine and of GlutQui (**3b**) responsible for 50% decrease of infected cell numbers were 0.68 μM and 15 μM , respectively.

We have realized that the prion healing curves for GlutQui (**3b**) are almost independent of the use of freshly prepared stock solution or aged stock solution. This opened a question whether the continuous treatment of infected cells in culture is necessary or only the first dose is responsible for the anti-prion effect. We have investigated it in more detail for FDA approved drug

quinacrine (Figure 6). Our results suggest that one dose of quinacrine (3 μM) can lead to complete disappearance of prion infected cells from culture; however, the continuous treatment was more effective in lowering the proportion of infected cells at lower quinacrine concentrations.

The healing of infected cells from prion infection with quinacrine and GlutQui (**3b**) including one dose mechanisms was confirmed by western blot (Figure 7). Complete loss of signal of PrP^{Sc} during continuous treatment was observed at 2 μM or 30 μM concentration of quinacrine or GlutQui (**3b**), respectively. For one dose treatment, the loss of signal of PrP^{Sc} was achieved at 3 μM or 50 μM concentration of quinacrine or GlutQui (**3b**), respectively. This shift of healing capabilities correlated well with the 20-fold lower affinity of GlutQui (**3a**) toward prion protein compared to quinacrine. The decrease of efficacy during one dose treatment was also observed in SSCA assay.

4. Discussions

The ability of 9-aminoacridines to react with thiol nucleophiles is well recognized (35,36). We and others previously shown (20,35,37) that quinacrine reacts also with GSH – quite abundant biological thiol nucleophile present in human body. Depletion of cellular GSH was observed during the treatment of cancer cell lines with 9-aminoacridine-thiazolidine derivatives (38). The reactivity of 9-aminoacridine derivatives with GSH could be directly responsible for GSH depletion. In our hands quinacrine reacted easily with GSH producing GlutQui, but unsubstituted 9-aminoacridine was stable toward GSH. The stability of unsubstituted 9-amino group towards nucleophilic substitution is in accordance with the stability of 9-aminoacridines towards nitrogen nucleophiles (27).

In order to test biological and physicochemical properties of GlutQui, we have developed a semi-large scale synthesis procedure. In contrast to previously published small-scale synthesis protocol (20) requiring HPLC purification of a reaction mixture the new separation strategy using ionex chromatography provides hundreds of milligrams of the peptide conjugate allowing to carry out biological and physicochemical assays. By working with higher amount of GlutQui, we also have realized that the conjugate can decompose to acridone and that this decomposition is concentration dependent.

Regarding to anti-prion activity, we can assume that quinacrine, to be effective, have to interact with prion protein. We have previously observed discrepancy (20,27) between weak binding of quinacrine to truncated recombinant prion protein hPrP121-230 (K_D 4.6 mM) (39) and strong anti-prion activity of quinacrine *in-vitro* (EC_{50} 0.3 μ M) (5,9). However, when prion protein spanning from 90 to 231 amino acids is used (hPrP90-231), more potent binding appeared (K_D 0.49 μ M) (24). Removal of ca 30 amino acids containing cluster of charged residues and part of the hydrophobic core of the protein led to totally different K_D values. The later reported K_D correlated well with the described anti-prion activity. Therefore, we applied the described assay for assessment of binding affinity of quinacrine and GlutQui to more accurate model – full-length His-mPrP23-231. In this assay, the conjugation with GSH led to 95% deactivation of quinacrine. Consequently we showed that the GlutQui conjugate is more than 3-times weaker prion protein binder than unsubstituted 9-aminoacridine. Whereas 9-aminoacridine is weaker binder than quinacrine, it is stable towards GSH. Thus, after quinacrine deactivation, 9-aminoacridine is 3-fold more potent prion protein binder than GSH deactivated quinacrine.

9-Aminoacridines are quite strong DNA binders. Tight binding to DNA severely limits the extravascular distributive properties of drugs, because diffusion is driven by the free drug concentration (2). For these compounds, the effective diffusion coefficient (D_{eff}) that rules the rate of extravascular diffusion, is significantly lowered by DNA binding and correlates with dissociation constant. It is given by $D_{eff} = \frac{D}{1 + \frac{S_f}{K_D}}$, where D stands for the diffusion coefficient, K_D is the DNA dissociation constant and S_f corresponds to the concentration of available DNA-binding sites (2). For a total DNA-binding site concentration of about 1 mM and non-specific binder (about 10% of the sites in chromatin), the lower limit of K_D to maintain the diffusion time useful on the pharmacological timescale is about 100 μ M (2). Thus, even quite moderate DNA binding limits diffusion of would-be drug. For 9-aminoacridines, the dissociation constants are in 10 μ M levels and their bioavailability is quite low. In some cases, the conjugation of 9-aminoacridines with peptides can increase acridine bioavailability by suppression of their DNA binding (40). However, when GSH accepts acridine moiety from quinacrine, the DNA affinity increases ca 5-folds (Table 2). We showed that the GlutQui conjugate is ca 21-times tighter binder than 9-aminoacridine. Thus, GSH not only suppresses prior binding of quinacrine but also decreases its bioavailability by enhanced DNA binding.

Another factor influencing bioavailability of drugs in human body is distribution coefficient $\log P$ between *n*-octanol—water (25), where *n*-octanol serves as a model of biological membranes. For polyelectrolytes such as peptides, the better measure is $\log D_{pH 7.4}$, where instead of pure water, the aqueous physiological buffer is used with pH 7.4 (26). The compounds with $\log D_{pH 7.4}$ in range -0.5 – 3 belong to families of most used drugs (41-44), i.e. they have well balanced membrane permeability and aqueous solubility in biological systems. Conjugation of GSH with quinacrine made the drug more water soluble and suppressed its membrane

permeability. Since prions in infected cells are located both on the cytoplasmic membrane and intracellularly (45), the hydrophilization of acridine moiety decreased approximately 100-fold local concentration of the active drug in prion active sites.

Toxicity of tested drugs also has to be taken in to the account. Toxic effect, presented as inhibition of cell division, of quinacrine or GlutQui occurred in concentration dependent manner. According to LC_{50} values in CAD5 cells, quinacrine is ca 80 times more toxic than GlutQui. Effectivity of treatment tested on RML infected CAD5 cell by SSCA have shown 25-fold decrease of GlutQui anti-prion activity compared to quinacrine. This observation corresponds to lower binding affinity of GlutQui to His-mPrP23-231. The activities of fresh and aging GlutQui stock solutions in SSCA cannot be explained by higher efficacy of formed acridone, because acridone **4** in saturated solution has only minor effect on number of prion infected cells in SSCA assay (Figure S2), which is in range of standard error of the assay (32). To simulate the drug regimen of aging GlutQui using quinacrine we treated infected cells only ones. We used only one dose at the first day of the assay. The similar effect of “only the first dose of drug heals the cells” appeared also for quinacrine. One dose of quinacrine (3 μ M) can lead to complete disappearance of prion infected cells from culture. Healing of prion infection by application of one dose only can indicate that acridines may (I.) either actively accumulate in the cells in concentration that is sufficient for prion removal even after its dilution by cell divisions; (II.) or can somehow reset the susceptibility of the cells to prion infection for at least several cell divisions enough for disappearance of PrP^{Sc} from the culture. This is supported by fact that the culture is growing exponentially after application and the medium is replaced every day with acridine-free system. It suggests that the cell divisions in combination with the initial impact of

acridines rather than permanent presence of acridines in media are necessary for healing of cells from the prion infection. Moreover, it could be also an explanation why the quinacrine anti-prion activity is effective only in replicating cell culture (15).

5. Conclusions

The exposure of quinacrine drug towards biogenic thiol – GSH – led to formation of acridine-peptide conjugate, which has 20-fold lower affinity toward recombinant prion protein. This biophysical parameter correlates well with 15-times lower anti-prion activity of GlutQui confirmed by western-blot and 25-fold decrease of anti-prion activity in standard scrapie cell assay. Moreover, GlutQui is 100-times more hydrophilic and 5-times more powerful dsDNA binder than the parent drug. Taking into account these findings, by conversion of quinacrine to the peptide-conjugate, we can estimate ca 2,000 times (20 x 100) lowering of activity in experiments *in-vivo* than that *in-vitro*. Moreover, the conjugate slowly decomposes to acridone, which is practically insoluble in water. However, the findings of our study should be interpreted cautiously as *in vitro* models utilized may imperfectly replicate complex *in vivo* situation.

Interestingly, it seems that acridines can heal prion infection of cultured cells by application of one dose only. Since from that time the culture is growing and the medium exchanged, most probably, the acridines have to either influence prion propagation by attacking the replication mechanism at the beginning of the treatment, or accumulate into the cells in concentration much higher than that required for treatment with subsequent dilution to lower but still effective concentration during cell replication.

Biological activity of 9-aminoacridines, which react with GSH, can be altered. It seems that acridines having 9-amino group without other substituents (primary amine) are resistant towards reaction with GSH. Thus, we hypothesize that new drugs can be designed as 9-aminoacridines with introduction of aminoalkyl chains in different positions than C-9. By this, they will be supposedly inert toward GSH.

Acknowledgments

We thank Prof. Charles Weissmann (SCRIPPS, Florida) and Prof. Vladka Curin-Serbec (Blood Transfusion Centre of Slovenia, Ljubljana) for the donation of materials. This work was supported by grants of the Czech Science Foundation (GA CR) No. 14-00431S; 15-09072S; 16-00270S; P303/12/1791; and Research Project RVO 61388963. TM, ED and KH were supported by projects of Charles University in Prague: PRVOUK-P24/LF1/3, UNCE 204022 and SVV 260026.

Conflict of interest: Authors declare that they have no conflict of interests.

References

1. Demeunynck, M., Charmantray, F., Martelli, A. (2001) Interest of acridine derivatives in the anticancer chemotherapy. *Curr Pharm Des* 7:1703-1724.
2. Denny, W. A. Acridine-4-carboxamides and the concept of minimal DNA intercalators, in: Demeunynck, M., Bailly, C., Wilson, W.D. editors. *Small molecule DNA and RNA binders*, Wiley-VCH Verlag GmbH & Co, Weinheim, 2003; p 482-502.
3. Šebestík, J., Hlaváček, J., Stibor, I. (2007) A role of the 9-aminoacridines and their conjugates in a life science. *Curr Prot Pept Sci* 8:471-483.

4. Wallace, D. J. (1989) The use of Quinacrine (Atabrine) in rheumatic diseases - a reexamination. *Seminars in Arthritis and Rheumatism* 18:282-297.
5. Korth, C., May, B. C. H., Cohen, F. E., Prusiner, S. B. (2001) Acridine and phenothiazine derivatives as pharmacotherapeutics for prion disease, *Proc Natl Acad Sci USA* 98:9836-9841.
6. Krauth-Siegel, R. L., Bauer, H., Schirmer, H. (2005) Dithiol proteins as guardians of the intracellular redox milieu in parasites: Old and new drug targets in Trypanosomes and Malaria-causing Plasmodia. *Angew Chem Int Ed* 44:690-715.
7. Saravanamuthu, A., Vickers, T. J., Bond, C. S., Peterson, M. R., Hunter, W. N., Fairlamb, A. H. (2004) Two interacting binding sites for Quinacrine derivatives in the active site of Trypanothione reductase. A template for drug design. *J Biol Chem* 279:29493-29500.
8. Burnett, J. C., Schmidt, J. J., Stafford, R. G., Panchal, R. G., Nguyen, T. L., Hermone, A. R., Vennerstrom, J. L., McGrath, C. F., Lane, D. J., Sausville, E. A., Zaharevitz, D. W., Gussio, R., Bavari, S. (2003) Novel small molecule inhibitors of Botulinum neurotoxin A metalloprotease activity. *Biochem Biophys Res Commun* 310:84-93.
9. May, B. C. H., Fafarman, A. T., Hong, S. B., Rogers, M., Deady, L. W., Prusiner, S. B., Cohen, F. E. (2003) Potent inhibition of Scrapie prion replication in cultured cells by bis-acridines, *Proc Natl Acad Sci USA* 100:3416-3421.
10. Bolognesi, M. L., Cavalli, A., Valgimigli, L., Bartolini, M., Rosini, M., Andrisano, V., Recanatini, M., Melchiorre, C. (2007) Multi-target-directed drug design strategy: From a dual binding site Acetylcholinesterase inhibitor to a trifunctional compound against Alzheimer's Disease. *J Med Chem* 50:6446-6449.

11. Collinge, J., Gorham, M., Hudson, F., Kennedy, A., Keogh, G., Pal, S., Rossor, M., Rudge, P., Siddique, D., Spyer, M., Thomas, D., Walker, S., Webb, T., Wroe, S., Darbyshire, J. (2009) Safety and efficacy of Quinacrine in human prion disease (PRION-1 study): A patient-preference trial. *Lancet Neurol* 8:334-344.
12. Geschwind, M. D., Kuo, A. L., Wong, K. S., Haman, A., Devereux, G., Raudabaugh, B. J., Johnson, D. Y., Torres-Chae, C. C., Finley, R., Garcia, P., Thai, J. N., Cheng, H. Q., Neuhaus, J. M., Forner, S. A., Duncan, J. L., Possin, K. L., Dearmond, S. J., Prusiner, S. B., Miller, B. L. (2013) Quinacrine treatment trial for sporadic Creutzfeldt-Jakob disease. *Neurology* 81:2015-2023.
13. Collins, S. J., Lewis, V., Brazier, M., Hill, A. F., Fletcher, A., Masters, C. L. (2002) Quinacrine does not prolong survival in a murine Creutzfeldt-Jakob Disease model, *Ann Neurol* 52:503-506.
14. Gayraud, V., Picard-Hagen, N., Viguié, C., Laroute, V., Andréoletti, O., Toutain, P. L. (2005) A possible pharmacological explanation for quinacrine failure to treat prion diseases: pharmacokinetic investigations in a ovine model of scrapie. *British J Pharmacol* 144:386-393.
15. Ghaemmaghami, M. S., Ahn, M., Lessard, P., Giles, K., Legname, G., DeArmond, S. J., Prusiner, S. B. (2009) Continuous Quinacrine treatment results in the formation of drug-resistant prions. *PLoS Pathogens* 5: art. no. e1000673.
16. Bian, J., Kang, H.-E., Telling, G. C. (2014) Quinacrine promotes replication and conformational mutation of chronic wasting disease prions. *Proc Natl Acad Sci USA* 111:6028-6033.

17. Ahn, M., Ghaemmaghami, S., Huang, Y., Phuan, P.-W., May, B. C. H., Giles, K., DeArmond, S. J., Prusiner, S. B. (2012) Pharmacokinetics of Quinacrine Efflux from Mouse Brain via the P-glycoprotein Efflux Transporter. *PLoS One* 7: art. no. e39112.
18. Yung, L., Huang, P. Y., Lessard, P., Legname, G., Lin, E. T., Baldwin, M., Prusiner, S. B., Ryou, C., Guglielmo, B. J. (2004) Pharmacokinetics of Quinacrine in the treatment of prion disease. *BMC Infectious Diseases* 4: art no 53.
19. Barret, A., Tagliavini, F., Forloni, G., Bate, C., Salmona, M., Colombo, L., De Luigi, A., Limido, L., Suardi, S., Rossi, G., Auvré, F., Adjou, K. T., Salčs, N., Williams, A., Lasmézas, C., Deslys, J. P. (2003) Evaluation of quinacrine treatment for prion diseases. *J Virol* 77:8462-8469.
20. Zawada, Z., Šafařík, M., Dvořáková, E., Janoušková, O., Březinová, A., Stibor, I., Holada, K., Bouř, P., Hlaváček, J., Šebestík, J. (2013) Quinacrine reactivity with prion proteins and prion-derived peptides. *Amino Acids* 44:1279-1292.
21. Hannaoui, S., Maatouk, L., Privat, N., Levavasseur, E., Faucheux, B. A., Haïk, S. (2013) Prion Propagation and Toxicity Occur In Vitro with Two-Phase Kinetics Specific to Strain and Neuronal Type. *J Virol* 87:2535-2548.
22. Guitart, K., Loers, G., Schachner, M. and Kleene, R. (2015) Prion protein regulates glutathione metabolism and neural glutamate and cysteine uptake via excitatory amino acid transporter 3. *J Neurochem* 133: 558–571.
23. Pavlíček, A., Bednářová, L., Holada, K. (2007) Production, purification and oxidative folding of the mouse recombinant prion protein. *Folia Microbiol (Praha)* 52:391-397.

24. Villa, V., Tonelli, M., Thellung, S., Corsaro, A., Tasso, B., Novelli, F., Canu, C., Pino, A., Chiovitti, K., Paludi, D., Russo, C., Sparatore, A., Aceto, A., Boido, V., Sparatore, F., Florio, T. (2011) Efficacy of novel acridine derivatives in the inhibition of hPrP90-231 prion protein fragment toxicity. *Neurotox Res* 19: 556-574.
25. Leo, A., Hansch, C., Elkins, D. (1971) Partition coefficients and their uses. *Chem Rev* 71:525-616.
26. Rubas, W., Cromwell, M. E. M. (1997) The effect of chemical modifications on octanol/water partition (log D) and permeabilities across Caco-2 monolayers. *Adv Drug Deliv Rev* 23:157-162.
27. Šebestík, J., Šafařík, M., Stibor, I., Hlaváček, J. (2006) Acridin-9-yl exchange: A proposal for the action of some 9-aminoacridine drugs. *Biopolymers (Pept Sci)* 84:605-614.
28. Šebestík, J., Hlaváček, J., Stibor, I. (2006) Rational design and synthesis of a double-stranded DNA-binder library. *Biopolymers (Pept Sci)* 84:400-407.
29. Luedtke, N. W., Liu, Q., Tor, Y. (2003) RNA-Ligand Interactions: Affinity and Specificity of Aminoglycoside Dimers and Acridine Conjugates to the HIV-1 Rev Response Element. *Biochem* 42:11391-11403.
30. Qi, Y., Wang, J. K., McMillian, M., Chikaraishi, D. M. (1997) Characterization of a CNS cell line, CAD, in which morphological differentiation is initiated by serum deprivation. *J Neurosci* 17:1217-1225.
31. Janoušková, O., Rakušan, J., Karásková, M., Holada, K. (2012) Photodynamic inactivation

of prions by disulfonated hydroxyaluminium phthalocyanine. *J Gen Virol* 93:2512-2517.

32. Mahal, S. P., Demczyk, C. A., Smith, E. W. Jr, Klohn, P. C., Weissmann, C. (2008) Assaying prions in cell culture: the standard scrapie cell assay (SSCA) and the scrapie cell assay in end point format (SCEPA). *Methods in Molecular Biology* 459:49-68.

33. Polymenidou, M., Verghese-Nikolakaki, S., Groschup, M., Chaplin, M. J., Stack, M. J., Plaitakis, A., Sklaviadis, T. (2002) A short purification process for quantitative isolation of PrP^{Sc} from naturally occurring and experimental transmissible spongiform encephalopathies. *BMC Infectious Diseases* 2:art no 23.

34. Panigaj, M., Glier, H., Wildova, M., Holada, K. (2011) Expression of prion protein in mouse erythroid progenitors and differentiating murine erythroleukemia cells. *PLoS One* 6: art no e24599.

35. Wild, F., Young, J. M. (1965) The reaction of Mepacrine with thiols. *J Chem Soc* 7261-7274.

36. Weltrowski, M., Ledochowski, A., Sowinski, P. (1982) Research on tumor-inhibiting compounds 70. Reactions of 1-nitroacridines with ethanethiol. *Polish J Chem* 56: 77-82.

37. Zawada, Z., Šebestík, J., Šafařík, M., Krejčířková, A., Březinová, A., Hlaváček, J., Stibor, I., Holada, K., Bouř, P. (2010) What could be the role of Quinacrine in Creutzfeldt-Jakob Disease treatment? in: Lebl, M. Meldal, M., Jensen, K., Hoeg-Jensen, T. editors, *Peptides 2010. Proc. 31st Eur. Pept. Symp., Eur. Pept. Soc.: Copenhagen DK*, p 84-85.

38. Paulíková, H., Vantová, Z., Hunáková, Ľ., Čížeková, L., Čarná, M., Kožurková, M.,

- Sabolová, D., Kristian, P., Hamul'aková, S., Imrich, J. (2012) DNA binding acridine-thiazolidinone agents affecting intracellular glutathione. *Bioorg Med Chem* 20:7139-7148.
39. Vogtherr, M., Grimme, S., Elshorst, B., Jacobs, D. M., Fiebig, K., Griesinger, C., Zahn, R. (2003) Antimalarial drug Quinacrine binds to C-terminal helix of cellular prion protein. *J Med Chem* 46:3563-3564.
40. Šebestík, J., Stibor, I., Hlaváček, J. (2006) New peptide conjugates with 9-aminoacridine: synthesis and binding to DNA. *Journal of Peptide Science* 12:472-480.
41. Zhu, C., Jiang, L., Chen, T.-M., Hwang, K.-K. (2002) A comparative study of artificial membrane permeability assay for high throughput profiling of drug absorption potential. *Eur J Med Chem* 37:399-407.
42. Hill, A. P., Young, R. J. (2010) Getting physical in drug discovery: a contemporary perspective on solubility and hydrophobicity. *Drug Discovery Today* 15:648-655.
43. Ungell, A.-L., Nylander, S., Bergstrand, S., Sjöberg, Å., Lennernäs, H. (1998) Membrane Transport of Drugs in Different Regions of the Intestinal Tract of the Rat. *J Pharmaceut Sci* 87:360-366.
44. Kansy, M., Senner, F., Gubernator, K. (1998) Physicochemical High Throughput Screening: Parallel Artificial Membrane Permeation Assay in the Description of Passive Absorption Processes. *Journal of Medicinal Chemistry* 41:1007-1010.
45. Prusiner, S. B. (1998) *Proc Natl Acad Sci USA* 95:13363-13383.

Supporting Information

Supporting information for this article contain figures: **Figure S1** Decomposition of **3b** to GSH (**2**) and acridone (**4**); **Figure S2** SSCA and western blot of acridone (**4**); **Figure S3** Copy of NMR spectrum of purified GlutQui (**3a**); **Figure S4** Copy of NMR spectra of purified GlutQui (**3b**); **Figure S5** Copy of NMR spectra of GlutQui after decomposition to GSH (**2**) and acridone (**4**); **Figure S6** Copy of HRMS spectra of GlutQui (**3a**); **Figure S7** Copy of HRMS spectrum of GlutQui (**3b**).

Figure legends

Figure 1 Reaction of FDA approved drug quinacrine (**1**) with GSH (**2**). GlutQui (**3**) is formed.

The GlutQui is quite unstable and slowly decompose to starting GSH (**2**) and corresponding acridone (**4**), which is practically insoluble in water.

Figure 2 Normalized ^1H -NMR spectra of acridine systems, peptide amides, and ammonium salts of GlutQui (**3b**) and decomposition mixture containing acridone (**4**) and GSH (**2**) using CryoProbe. At the top spectrum of freshly prepared solution with low concentration of **3b** in order to prevent decomposition of the sample. The bottom represents acridone (**4**) and GSH (**2**) spectrum obtained after complete decomposition. In the figure, only aromatic H are assigned, for full assignment see also section 2.4. Spectra showing the progress of decomposition at high concentration of **3b** are depicted in Figure S1 in supplementary materials.

Figure 3 Förster resonance transfer assay for determination of acridine-prion protein binding.

Quinacrine (X,---), 9-aminoacridine (*, ---), GlutQui (**3a**, +, ---).

Figure 4 Toxicity of quinacrine (left) and GlutQui (**3b**, right) to CAD5 cells in culture. Each concentration was tested in two independent experiments (black and red). LC_{50} values were 1.3 and $\geq 97 \mu\text{M}$ for quinacrine and GlutQui (**3b**), respectively.

Figure 5 The effect of quinacrine and GlutQui (**3b**) treatment on prion clearance from infected CAD5 cells was evaluated by SSCA. Each point represents the mean from 8 values. Concentrations were tested in two independent experiments (black and red; green and magenta). In case of GlutQui, black and red represent treatment with aging stock solution i.e. contaminated with acridone after the GlutQui decomposition. Green and magenta stand for application of freshly prepared stock solution. Unfortunately, fresh GlutQui at higher concentration prevented SSCA by formation of yellow spots on ELISPOT plate. EC_{50} values were 0.68, 15, and 15 μM for quinacrine, aging GlutQui, and fresh GlutQui, respectively.

Figure 6 The effect of continuous and one dose quinacrine treatment on prion clearance from infected CAD5 cells detected by SSCA. The green and blue circles represent the continuous treatment with quinacrine, where the fresh solution of quinacrine was added daily after every change of media. The brown and orange squares stand for one dose treatment, with quinacrine added only once at the beginning of the experiment. Each point represents the mean from 8 values. Concentrations were tested in two independent experiments (replicate 1 (green and orange) and replicate 2 (blue and brown)). From the fitting, the EC_{50} values for continuous and one dose treatments were 0.68 and 1.1 μM , respectively.

Figure 7 Elimination of abnormal prion protein from RML infected CAD5 cells detected by western blot. RML infected CAD5 cells were treated with different concentrations of quinacrine (A every day, B only one dose) or GlutQui (**3b**, C every day, D only one dose) for 7 days. Cells

were harvested and the presence of cellular prion protein (PrP^C)/PrP^{Sc} detected by western blot.

Non-infected cells (CAD5) were used as a control. Samples without PK treatment contain both PrP^C and PrP^{Sc}. Samples treated with PK (PK+) contain proteinase resistant pathological PrP^{Sc}.

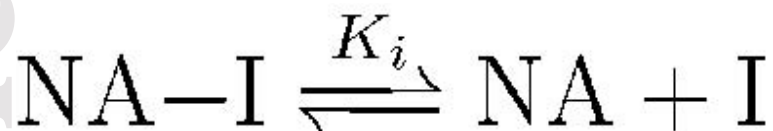
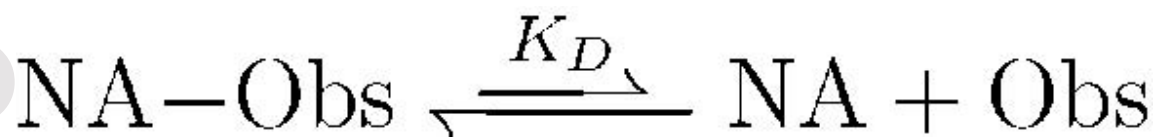
Blots are representative of two independent experiments.

$$D_{eff} = \frac{D}{1 + \frac{S_f}{K_D}}$$

$$F = (F_{max} - F_{\infty}) * \exp\left(\frac{-0.69}{QC_{50}} C\right) + F_{\infty}$$

$$\frac{1}{\Delta F} = \frac{F_{max} - F_{\infty}}{F - F_{\infty}}$$

$$\frac{1}{\Delta F} = \frac{F_{max} * K_D}{c_{Lig}} + c_{Lig}$$



$$K_i = \frac{K_D * [\text{NA-Obs}] * [\text{I}]}{[\text{Obs}] * [\text{NA-I}]}$$

Table 1 Acridine-prion protein binding parameters.

Compound	QC_{50} [μM] ^a	K_D [μM]
quinacrine	20.8	0.17
9-aminoacridine	125	1.08
GlutQui (3a)	414	3.49

^athe concentration of acridine compounds causing 50% quenching of prion protein fluorescence.

Table 2 Acridine-dsDNA binding evaluated by competitive ethidium bromide assay

Compound	IC_{50} [μM] ^a	K_i [μM] ^b
quinacrine	19.1	14.1
9-aminoacridine	87.9	65.2
GlutQui (3a)	4.29	3.12

^aConcentration of acridine compound causing 50% inhibition of ethidium binding to dsDNA.

^bApparent inhibition constant of ethidium-dsDNA binding with acridines based on ethidium binding parameters K_D 0.88 μM and n 0.464 in base-pairs.

Table 3 Partition coefficient between two phases: n-octanol-phosphate buffer pH 7.4

Compound	$\log D_{pH\ 7.4}$
quinacrine	0.41
9-aminoacridine	0.65
GlutQui (3a)	-1.60

Table 4 Solubility of acridines

Compound	Solubility [mg/mL]
Quinacrine . 2HCl	40 ^a
9-aminoacridine . HCl	61 ^a
GlutQui . 2 TFA	45 ^a
GlutQui . 2 AcOH (3a)	720 ^{a,b}
GlutQui . 9/4 HCl . 9/4 H ₂ O (3b)	0.2 ^{a,c}
GlutQui. 9/4 HCl . 9/4 H ₂ O (3b)	> 50 ^d
2-methoxy-6-chloroacridin-9-one	< 0.000303 ^e

^aSolubility in water

^bVery viscous, honey-like solution

^cAbove this concentration, solid-gel formation

^dSolubility in DMSO

^e0.91 mg was not soluble in 3 L of water, detected by luminescence at 365 nm

